Four-Component Relativistic Coupled Cluster and Configuration Interaction Calculations on the Ground and Excited States of the RbYb Molecule†

Lasse Kragh Sørensen,‡ Stefan Knecht,† Timo Fleig,*,‡,§ and Christel M. Marian*,‡

Institute of Theoretical and Computational Chemistry, Heinrich Heine University Düsseldorf, Düsseldorf, Germany

Received: May 26, 2009; Revised Manuscript Received: July 29, 2009

We present high-level four-component coupled cluster and multireference configuration interaction calculations of potential energy curves, dipole moment, Franck−Condon factors and spectroscopic constants of the newly formed RbYb molecule. From finite-field calculations we obtain an electric dipole moment for RbYb of almost 1 D. In combination with its magnetic dipole moment this makes RbYb an excellent candidate for trapping and for studying dipolar interaction in the ultracold regime. Significant Franck−Condon factors are found between the rovibronic ground state and the lowest rovibrational levels of the first excited $^2\Sigma^+_{1/2}$ state but also between a broad range of rovibrational levels of the $^2\Pi_{1/2}$ and $^2\Pi_{3/2}$ states. This allows for several two-step approaches to reach the rovibronic ground state after initial photoassociation.

1. Introduction

A number of groundbreaking achievements has been reported from the field of cold and ultracold molecules, and ongoing investigations bear the potential for yet further findings of fundamental importance.[1] These range from the production of Bose−Einstein condensates (BECs)[2] to the striving for a controlled chemistry at the quantum level[3] and the possibility of testing, e.g., fundamental symmetries in nature through measurements of a postulated electric dipole moment (EDM) of an electron[4,5] or the space−time variation of fundamental constants such as the fine-structure constant α.[6,7] The experimental work for producing (ultra)cold molecules has to the date been conducted in a variety of ways, such as photoassociation (PA),[8] buffer gas cooling (sympathetic cooling),[9] Stark deceleration of polar molecules via time-modulated electric fields,[10] and magnetically tunable Feshbach resonances.[11]

Theoretical contributions to the field of (ultra)cold molecules are of value in many different respects. Among the most important is the determination of accurate molecular potential energy curves (PECs) of ground and relevant electronically excited states. These potentials are often required to be known at both short and long range.[8] At long-range, atom−atom interactions are typically evaluated by perturbation theory, whereas at short range advanced methods of molecular electronic structure theory come into play. In addition to the spectral constants which may be extracted directly from the short-range potentials (equilibrium bond lengths, harmonic vibrational frequencies, dissociation, and excitation energies),[12−14] vibrational states and Franck−Condon factors (FCFs),[15] molecule formation rates,[16] and electric properties such as permanent EDM,[17,18] transition dipole moments,[19] and static polarizabilities are of interest and have been determined by theoretical methods.

A large fraction of investigated systems in the (ultra)cold molecular sciences is composed of alkali metal diatomics. The RbYb molecule belongs to a new class of heteronuclear diatomics that due to their unpaired electron(s) may be trapped and manipulated using magnetic fields.[20] They are, for example, promising candidates for an experimental search for a permanent electric dipole moment of the electron or for producing lattice-spin models[21] for quantum computing. Recently, the thermalization of various bosonic and fermionic Yb isotopes through collisions with ultracold Rb has been shown, giving first insights into the long-range behavior of the RbYb potential.[22] On the basis of this work, the controlled production of electronically excited RbYb* molecules by single-photon photoassociation techniques has been demonstrated,[20] and continued efforts include the conservative trapping of the Rb−Yb mixture. Ultimately, the investigations aim at a molecular BEC with adjustable dipolar interaction and a new approach to measuring the electron EDM. The prospects have motivated us to explore the electronic structure of the RbYb molecule with reliable and accurate relativistic electronic structure methods.

In this paper we present, to the best of our knowledge, the first theoretical investigation of the RbYb molecule. The focus of this investigation has been on a simultaneously accurate description of the ground and lowest electronically excited states and to propose possible ways for a photoassociation process leading to the rovibronic ground state. Since two heavy atoms are involved, we apply quantum-chemical methods that treat electron correlation and relativistic effects on the same footing. Relativistic coupled cluster and configuration interaction approaches are used in a complementary fashion, the details of which are described in the following section. In the main body of the paper (section 3) we outline a way of achieving high accuracy by first a systematic study of the ground and excited states of the atoms and, in addition, of the electronic ground state of the molecule. Based on these results, a final multireference (MR) CI model expansion is chosen that can deliver accurate spectroscopic values for the states in question. We present and discuss electronic molecular potentials obtained with this MRCI model and point to possible pathways to the rovibronic ground state based on the derived FCFs. We furthermore present the computed dipole moment function of the ground state showing that RbYb also possesses a substantial

† Part of the "Russell M. Pitzer Festschrift".

* E-mail: timo.fleig@irsamc.ups-tlse.fr; Christel.Marian@uni-duesseldorf.de.

‡ HHU Düsseldorf.

§ Permanent address: Laboratoire de Chimie et Physique Quantiques, I.R.S.A.M.C., Université Paul Sabatier, Toulouse, France.

10.1021/jp904914m CCC: $40.75
Published on Web 08/18/2009

electric dipole moment along with a magnetic dipole moment due to the unpaired electron. In the final section we summarize and draw conclusions.

2. Theory and Computational Details

2.1. Hamiltonian Operators. The spectroscopic properties of RbYb are expected to be significantly influenced by relativistic effects and electron correlation. For the ground state $^2\Sigma^+_{1/2}$ scalar-relativistic effects cause a large contraction and stabilization of the 6s spinors on Yb and a smaller one of the 5s spinors on Rb. For the lowest excited states we expect a significant spin−orbit splitting for $Rb_{5p^1}(^2P_{3/2,1/2})$ and a large spin−orbit coupling (SOC) for $Yb_{6s^16p^1}(^3P_{2,1,0})$ and $Yb_{6s^16p^1}(^1P_1)$. We have therefore decided to carry out this theoretical investigation in the more rigorous 4-component framework using the Dirac−Coulomb (DC) Hamiltonian for calculations including excited states and Dyall's spinfree Hamiltonian[23] for ground-state-only calculations. To correctly describe the SOC of the excited states, the DC Hamiltonian suffices since it contains the leading spin−orbit terms for heavy elements, namely the one-electron spin−orbit and the two-electron spin−same-orbit terms. The effect of the spin−other-orbit term, which is derived from the Gaunt operator and is therefore not included in the DC Hamiltonian, has been examined at the SCF level. It was found that the change in the splitting of the $Rb_{5p}(P_{3/2,1/2})$ and $Yb_{6p}(P_{3/2,1/2})$ levels decreased by 0.72 and 19.8 cm^{-1}, respectively. This reduction amounts to a change for $Rb_{5p}(P_{3/2,1/2})$ of 1.7% and for $Yb_{6p}(P_{3/2,1/2})$ of 1%, which is still below the accuracy we can typically achieve for relative energies. Including the full Breit interaction has been shown to have only little influence on the excitation energies of Yb[24] and on the alkali metal atoms in general.[25]

2.2. Correlation Methods and Setup. For the study of ground-state spectroscopic and electric properties we employed the RELCCSD module[26,27] in the DIRAC quantum chemistry program package,[28] which can perform CCSD and CCSD(T) calculations. The dominant relativistic contributions to the ground state are scalar relativistic. We therefore applied Dyall's spinfree Hamiltonian[23] in the coupled cluster calculations. Dirac−Coulomb Hartree−Fock (DCHF) calculations were performed with an averaging of three electrons in two Kramers pairs (3in2) consisting of the Rb 5s and Yb 6s spinors. Additional test calculations were carried out in a spin-dependent framework employing either a (3in2) or (3in5) averaging. In the latter DCHF setup three electrons were distributed among five Kramers pairs consisting of the Rb 5s and Yb 6s6p spinors. These ground-state coupled cluster calculations served as a benchmark for the corresponding MRCI calculations.

The calculation of excited-state wave functions and vertical as well as adiabatic excitation energies has been performed with the relativistic large-scale MRCI program LUCIAREL.[29−31] Like in the CIDBG[32] and SOCI[33] in the COLUMBUS code, double group symmetry is used. The recent parallel implementation[34] of LUCIAREL has opened for the possibility to treat larger CI expansions (>10^8 determinants) within a reasonable time frame on standard Linux-based clusters which has also been demonstrated for the SOCI program.[35]

The CI program LUCIAREL operates on the basis of a fully variational treatment of any spin-dependent two- or four-component Hamiltonian that is available in the present developer version of the DIRAC package.[28] It furthermore takes advantage of the concept of generalized active spaces (GAS)[29] to define suitable orbital spaces thereby allowing for arbitrary occupation constraints. Molecular spinors based on a true two- or four-component framework can be obtained from all-electron self-consistent field (SCF), Kramers-restricted multiconfigurational self-consistent field (KR-MCSCF),[36] or natural MP2 spinor[37] calculations. The string-driven MRCI[29−31,38] as well as the MRCC[17,39−42] methods are an alternative to the Tensor Contraction Engine[43] in generation of higher-order methods or code for more complex calculations.

To obtain accurate excitation energies, the initial DCHF step was performed with a (3in5) averaging of states. A (3in8) averaging, where the Rb 5p spinors are included, was not possible along the entire potential energy curve due to strong mixing with the Yb 5d spinors. The Rb 5p spinors were, however, included in the correlation step in a (3in8) MRCI excitation scheme that is in the following dubbed as S6_(3in8)_SD. Our notation follows the scheme "GAS I_(GAS II)_GAS III" and is most easily explained by an example: "S6_(3in8)_SD" means that at most 1 hole among the 6 electrons in 3 Kramers pairs (in this case: Rb 4p spinors) is allowed, 3 electrons are distributed in 8 Kramers pairs in all possible ways (plus of course excitations from GAS I to GAS II), and finally that all possible single and double excitations into GAS III Kramers pairs are generated from the reference configurations obeying the constraints put on GAS I and GAS II. As discussed in more detail in section 3.1, the inclusion of the Rb 4p spinors is required in the correlation step to obtain a good description of the lowest three atomic channels.

In addition to our thorough investigation of the four lowest molecular electronic states of RbYb, we show in Figure 1 a qualitative picture of the low-lying molecular electronic spectrum including respective atomic dissociation channels. In these calculations, denoted as SDT3 which corresponds to a Full CI calculation with three electrons, we truncated the space of virtual spinors at 2.0 E_h. It should be noted that the $Rb_{4d^1}(^2D_{5/2,3/2})$ states should be below the $Yb_{6s^16p^1}(^3P_2)$ states in the atomic limit which is not the case here due to the choice of DCHF averaging.

As full linear symmetry is not available yet in the present LUCIAREL implementation the calculations, have been carried out in the Abelian sub double group C_2^*. The assignment of the Ω quantum number for each individual electronic state has been accomplished by means of calculating the expectation value for the one-electron operator $\hat{j}_z = \hat{l}_z + \hat{s}_z$. This option has become available with the very recent implementation of a general CI property module[44] capable of treating basically any one-electron operator that is implemented in the program package.[28]

2.3. Basis Sets and Number of Correlated Electrons. All calculations were performed using uncontracted basis sets. For the ground-state coupled cluster calculations the aug-cc-pVTZ basis set for Yb (30s24p16d13f4g2h)[45] from Gomes and Dyall was chosen. It includes correlating functions for outer- and inner-valence shells down to the Yb 4f and polarizing functions for these. For Rb (29s21p15d2f)[46] Dyall's aug-cc-pVTZ basis set, which includes correlating and polarizing functions down to Rb 4s4p, was used. For a description of the general procedure of how to derive these functions see for example ref 47. In the following this basis set will be referred to as (ext_bas).

The effect of changing the number of correlated electrons has been examined at the CCSD and CCSD(T) levels. Either nine electrons from the Rb 4p5s and Yb 6s spinors were treated explicitly in the correlation step or 23 electrons were used, where the Yb 4f spinors were then included in addition. As shown in sections 3.1 and 3.2, the differential effects of correlating the Yb 4f electrons were found to be minor. In contrast, the correlation of the Rb 4p electrons had significant impact on the energy separation of the atomic levels and on the equilibrium

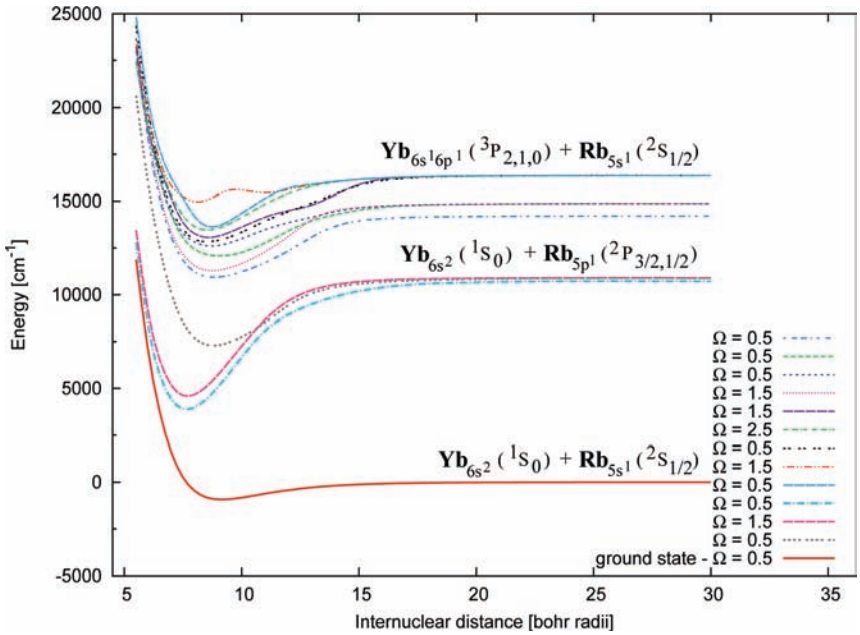

Figure 1. Qualitative picture of the potential energy curves of the molecular electronic states constituting the lower electronic spectrum of RbYb. Correlating atomic dissociation channels for the states are labeled. The computational level is CI SDT3 (see text for more details).

distance of the molecular ground state. We therefore decided to correlate nine electrons (Rb 4p5s and Yb 6s) in the MRCI calculations.

For the MRCI calculations the core-polarizing functions for both atoms were omitted since no electric properties were calculated. This reduced the size of the basis set (min_bas) to (30s24p16d13f3g1h) for Yb and (28s20p14d1f) for Rb. The truncation value for the virtual spinors in all correlated calculations was kept at 7.8 E_h since this threshold includes all polarizing functions and, in addition, was still tractable for the MRCI calculations. Spinors above this threshold are primarily core-correlating and will therefore only give minor contributions to valence spectroscopic values and electric properties.

2.4. Finite-Field Dipole Moment. The response of a molecular system to a weak external electric field ε can be treated as a perturbation to the field-free case. If the energy is expanded in a Taylor series around the field-free case

$$E(\varepsilon) = E(\varepsilon = 0) + \left.\frac{dE}{d\varepsilon}\right|_{\varepsilon=0} \varepsilon + \frac{1}{2}\left.\frac{d^2E}{d\varepsilon^2}\right|_{\varepsilon=0} \varepsilon^2 + \ldots \quad (1)$$

the first derivative of the energy E with respect to the external electric field ε taken at $\varepsilon = 0$ is the static dipole moment of the molecule. Likewise the second derivative can be related to the static polarizabilty and higher derivatives to higher-order (hyper)polarizabilities.

With the finite-field technique these analytical derivatives are approximated by a numerical derivative. To this end a small external electric field of varying field strength is applied and then a series of energy calculations is performed with these fields. By applying fields in various directions, we can also determine higher-order numerical derivatives, though these are not as accurate as the analytical ones.

The ground-state dipole moment was calculated by applying a finite electric field of varying strength along the bond axis (chosen as z). The field strengths considered here were ± 0.0001, ± 0.0002, and ± 0.0004 E_h e^{-1} bohr^{-1}. From these seven points a polynomial fit to the total field-dependent energy was made to find the numerical derivative and thereby also the dipole moment at a given internuclear distance. This was done at the CCSD and CCSD(T) levels of theory with 23 explicitly correlated electrons.

The advantage of the derivative technique is that it holds also for approximate wave functions, which are typically dealt with in quantum chemistry, unlike the evaluation of properties by calculating expectation values in the Hellmann−Feynman theorem, which differ from the correct value by the *wave function force*.[48]

2.5. Spectroscopic Values and Franck−Condon Factors. A polynomial fitting procedure with exponents ranging from −1 to +4 was used to fit the electronic ground- and excited-state potentials around their respective minima. Spectroscopic constants have then been determined by solving a one-dimensional Schrödinger equation of nuclear motion using a reduced mass calculated from isotopic abundance.[49] The harmonic frequency has been calculated from the second derivative at the minimum. Vibrational wave function, eigenvalues, and FCFs have been computed with the program LEVEL 8.0 by LeRoy.[15]

2.6. Counterpoise Correction. As RbYb is a van der Waals complex and therefore the ground state is very weakly bound by dispersion forces, the basis set superposition error (BSSE) may play a significant role in determining spectroscopic values even in large and balanced basis sets[50,51] due to the slow convergence toward basis set saturation. This artifact has been examined by a counterpoise (CP) correction, as suggested by Boys and Bernardi[52] for both ground and excited states, which is the correct way of evaluating differential quantities.[51,53,54] The BSSE is defined in the usual manner

$$\mathrm{BSSE}(R) = E^{A(AB)}(R) + E^{B(AB)}(R) - E^A - E^B \quad (2)$$

where $E^{A(AB)}(R)$ and $E^{B(AB)}(R)$ are the monomer energies obtained in the full dimer basis (AB) at a given distance (R) and E^A and E^B are the monomer energies in their respective basis. Every point on the potential energy curve is thereby CP corrected. The CP correction has been shown to be a very good estimate for the BSSE in medium to large basis sets and to

TABLE 1: Selection of Molecular Electronic States in the Λ−S Coupling Picture and Associated Atomic Dissociation Channels in an Energy Range of ≈25 000 cm^{-1} [a]

atomic $^{(2S+1)}L_J$	molecular $^{(2S+1)}\Lambda_\Omega$
$Rb_{5s^1}(^2S_{1/2}) + Yb_{6s^2}(^1S_0)$	$^2\Sigma 1/2 +$
$Rb_{5p^1}(^2P_{3/2,1/2}) + Yb_{6s^2}(^1S_0)$	$^2\Pi_{3/2,1/2}$, $^2\Sigma 1/2 +$
$Rb_{5s^1}(^2S_{1/2}) + Yb_{6s^16p^1}(^3P_{2,1,0})$	$^4\Pi_{5/2,3/2,1/2,-1/2}$, $^2\Pi_{3/2,1/2}$, $^4\Sigma 3/2,1/2 +$, $^2\Sigma 1/2 +$
$Rb_{4d^1}(^2D_{5/2,3/2}) + Yb_{6s^2}(^1S_0)$	$^2\Delta_{5/2,3/2}$, $^2\Pi_{3/2,1/2}$, $^2\Sigma 1/2 +$
$Rb_{6s^1}(^2S_{1/2}) + Yb_{6s^2}(^1S_0)$	$^2\Sigma 1/2 +$
$Rb_{5s^1}(^2S_{1/2}) + Yb_{6s^15d^1}(^3D_{3,2,1})$	$^4\Delta_{7/2,5/2,3/2,1/2}$, $^2\Delta_{5/2,3/2}$, $^4\Pi_{5/2,3/2,1/2,-1/2}$, $^2\Pi_{3/2,1/2}$, $^4\Sigma 3/2,1/2 +$, $^2\Sigma 1/2 +$
$Rb_{6p^1}(^2P_{3/2,1/2}) + Yb_{6s^2}(^1S_0)$	$^2\Pi_{3/2,1/2}$, $^2\Sigma 1/2 +$
$Rb_{5s^1}(^2S_{1/2}) + Yb_{6s^16p^1}(^1P_1)$	$^2\Pi_{3/2,1/2}$, $^2\Sigma 1/2 +$

[a] Molecular electronic states correlating to atomic channels with intra-atomic Yb f−d excitations, e.g., $Yb_{4f^{13}5d^16s^2}$ are not considered.

provide a smooth convergence of properties to the complete basis set limit.[55,56] Despite the apparent ease to eliminate a basis set incompleteness artifact one should, however, be careful in relying on this form of error compensation since a CP correction will not improve the overall basis.

3. Results and Discussion

3.1. Qualitative Molecular Electronic Spectrum and Atomic Calculations. Table 1 gives an overview over the atomic configurations and terms as well as the associated molecular states in the Λ−S coupling picture that are expected to form the lower part of the electronic spectrum of RbYb. The energetically close-lying valence-electronic Yb 6s and 6p shells as well as the valence-electronic Rb 5s and low-lying Rb 5p, 4d, 6s, and 6p shells suggest a large variety of excited states with angular momentum projection greater than zero within an energetic range of ≈25 000 cm^{-1}. As these states are affected by spin−orbit interaction to first order in a perturbation theory sense and as ytterbium is a heavy atom, the corresponding splittings and mixings are expected to be sizable. We provide in Figure 1 a qualitative survey of all molecular states correlating to the three lowest atomic channels listed in Table 1. Comparing the atomic-like excitation energies, computed at the CI SDT3 level of theory, with the experimentally available data, we find a large deviation of ≈2000−3000 cm^{-1} for the lowest P channels of both Rb and Yb. In contrast, the splitting among the various *J*-states is reproduced rather well. These results indicate that spin-dependent effects are taken into account properly whereas significant parts of the differential electron correlation are missing at this level of calculation. As we in the present study turn our main attention to the ground and three lowest excited states of RbYb, which are of particular importance for the experimental PA process,[20] we further investigated the effect of correlating the outer-core Rb 4p shell on the excitation energies. Since alkali atoms are known to have easily polarizable cores, we expect a considerable influence here.

Our calculated atomic and atomic-like excitation energies T_e for the lowest Rb 5s−5p transitions are compiled in Table 2 and atomic Yb 6s−6p transitions in Table 3. If core−valence polarization from the Rb 4p shell is neglected in the calculation of the lowest Rb 5s−5p transition, not only a considerable underestimation of the excitation energies of almost 2000 cm^{-1} is found, as indicated in Table 2 for the atomic S1 (one electron CI) and quasi-molecular SDT3 calculations, but also a too small fine-structure splitting of the ($^2P_{3/2,1/2}$) state of 183(2) cm^{-1} in comparison with the measured splitting of 237.6 cm^{-1}. However, taking into account single excitations from the outer-core Rb 4p shell (S6_(1in4)_SD) results in a significant improvement

TABLE 2: Atomic and Atomic-Like (Values Taken at R = 30 bohr) Excitation Energies T_e in cm^{-1} for the Lowest $Rb_{5s^1}(^2S_{1/2}) \rightarrow Rb_{5p^1}(^2P_{3/2,1/2})$ Transitions Calculated at the MRCI S1, S6_(1in4)_SD, SDT3, and S6_(3in8)_SD Levels, Respectively[a]

method/T_e (cm^{-1})	$J = 0.5$	$J = 0.5$	$J = 1.5$	
	$\Omega = 0.5$	$\Omega = 0.5$	$\Omega = 1.5$	$\Omega = 0.5$
S1	0	10692	10875	10875
S6_(1in4)_SD	0	12636	12857	12857
SDT3	0	10708	10890	10892
S6_(3in8)_SD	0	12662	12879	12883
experiment[59]	0	12578.95	12816.55	12816.55

[a] Details on the computational levels are given in the text.

TABLE 3: Atomic Excitation Energies T_e in cm^{-1} for the Lowest $Yb_{6s^2}(^0S_0) \rightarrow Yb_{6s^16p^1}(^3P_{2,1,0})$ Transitions Calculated at the MRCI S2, S14_(2in4)_SD, S20_(2in4)_SD and S20_(2in9)_SD Levels, Respectively[a]

method/T_e (cm^{-1})	$J = 0$	$J = 0$	$J = 1$	$J = 2$
S2	0	14209	14865	16362
S14_(2in4)_SD	0	15497	16164	17734
S20_(2in4)_SD	0	17233	17931	19611
S20_(2in9)_SD	0	17346	18034	19722
experiment[59]	0	17288.44	17992.01	19710.39

[a] Details on the computational levels are given in the text.

toward the experimental values. Excitation energies and the fine-structure splitting differ from the experimental data by about 40−60 cm^{-1} and 15 cm^{-1}, respectively.

What about T_e for the Rb 5p excitation computed at the quasi-atomic limit (R = 30 bohr) applying our MRCI S6_(3in8)_SD model? It can be seen from Table 2 that in the atomic limit the excitation energies are slightly shifted to higher energies by about 22−26 cm^{-1} yet yielding an excellent spin−orbit splitting of 218 cm^{-1}. The excitation energies are in very good agreement with the experimental data, exhibiting a maximum deviation of 83 cm^{-1} for the lower 2 0.5 state, and compare well to the two-component MRCI results of Lim et al.[57] using energy-consistent pseudopotentials. Furthermore, the energetic difference of only 4 cm^{-1} between the sublevels of the J = 1.5 atomic channel indicates that we are almost in the atomic limit at an internuclear distance of 30 bohr.

As a prospect for future studies on this system, we show our atomic MRCI calculations on the Yb atom where we studied the relevance of taking into account core−valence polarization from the Yb 4f and 5p shells. If only the two Yb 6s valence electrons are correlated (denoted as S2), transition energies for the respective Yb 6s−6p excitation are consistently too low by around 18%. The inclusion of the Yb 4f electrons in the correlation step (S14_(2in4)_SD) yields some improvement. However, only upon explicitly treating core−valence polarization from the Yb 5p shell (S20_(2in4)_SD) do we obtain excitation energies that are in good agreement with the experimental data. A further improvement is achieved by extending the active space to comprise the Yb 6s, 6p, and 5d shells (S20_(2in9)_SD). In this case, the deviations from the experimental values are less than 60 cm^{-1}, and the fine-structure splitting is very well reproduced.

Summarizing, the SDT3 level is insufficient for an accurate description even of the four lowest-lying dissociation channels (Rb 5s^1 + Yb 6s^2 and Rb 5p^1 + Yb 6s^2). It may thus be used only for obtaining a qualitative overview. In contrast, the S6_(3in8)_SD scheme reproduces the energetic splitting of these levels very well. Yb excitations do not play a major role in the

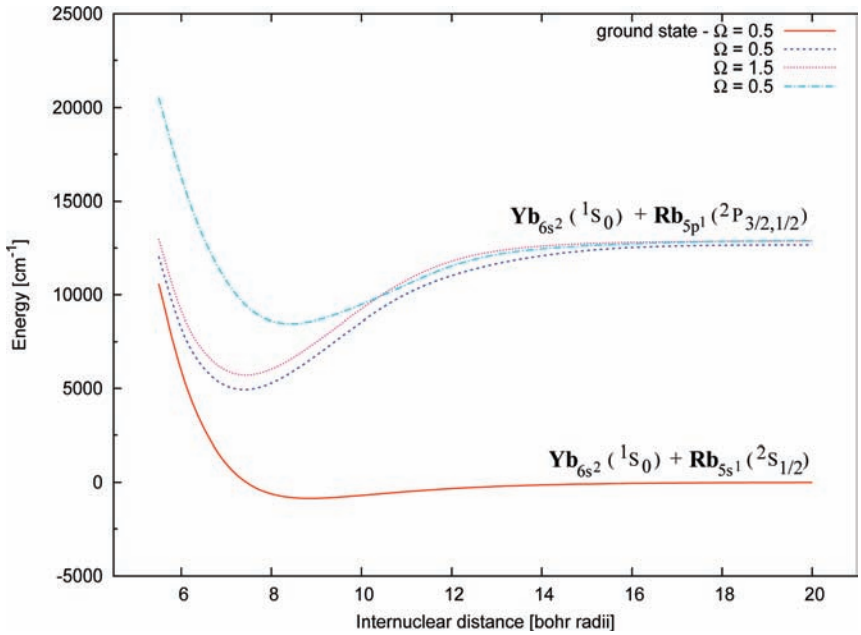

Figure 2. Potential energy curves of the four lowest-lying molecular electronic states of RbYb. Atomic dissociation channels for the states are shown. The computational level is S6_(3in8)_SD (see text for more details).

atomic channels that correlate with the four lowest-lying molecular states relevant for the PA process. We thus conclude that our chosen MRCI S6_(3in8)_SD model should provide a reliable description of the long-range behavior of these states in the RbYb molecule.

3.2. Ground-State Potential. The electronic ground state of RbYb exhibits a shallow potential shape (see Figure 2) that is a characteristic feature of a van der Waals molecule. Since the ground state is very sensitive to the DCHF averaging of the spinors and to the level of electron correlation, the simultaneously correct description of both ground and excited states becomes a complicated matter. Changes in the DCHF averaging or the correlation treatment can lead to large variations of the spectroscopic constants, here, in particular, the equilibrium bond distance. These differences may result in a substantial change of FCFs between ground and excited states.

We therefore first examined the ground state of RbYb with the coupled cluster method to provide a benchmark for the MRCI calculations. The aim here was to find the effect of outer-core polarization/correlation of the Yb 4f and Rb 4p. This has been done by varying the number of explicitly correlated electrons from 3 to 9 and to 23. Results of these calibration calculations are compiled in Table 4. Comparing those results, one sees that after a CP correction the effect of including the Rb 4p electrons on the bond length is more than 1 magnitude larger than including Yb 4f as the bond contracts from 9.18 bohr (CP-CCSD(T), 3 electrons correlated) to 8.94 bohr (CP-CCSD(T), 9 electrons correlated) and 8.93 bohr (CP-CCSD(T), 23 electrons correlated). The correlation of the Yb 4f electrons does, nevertheless, have an effect comparable to the inclusion of the Rb 4p electrons on the harmonic frequency and the dissociation energy in reducing both. These changes are, however, of little importance for the present investigation and, furthermore, the polarization of Yb 4f plays a minor role in the lowest-lying excited states for the molecule (see section 3.1). Therefore, we decided not to include the Yb 4f in the MRCI calculations. Another reason to omit the Yb 4f is the large CP correction, which shows that with this particular basis set and truncation of virtuals we did not yet come close enough to basis set saturation for the Yb 4f shell. The otherwise minor CP correction for the 3 and 9 electron CCSD and CCSD(T) calculations indicates that we have a balanced basis set.

TABLE 4: Spectroscopic Values for the 1 0.5 Ground State Calculated at the CCSD and CCSD(T) Level with 3, 9, and 23 Explicitly Correlated Electrons and with CP Corrected Values

method	corr el	R_e (bohr)	ω_e (cm^{-1})	D_e (cm^{-1})
CCSD-SF	3	9.30	26.278	606
CP-CCSD-SF	3	9.30	26.257	605
CCSD(T)-SF	3	9.18	28.941	818
CP-CCSD(T)-SF	3	9.18	28.923	816
CCSD-SF	9	9.20	24.814	600
CP-CCSD-SF	9	9.22	24.554	588
CCSD(T)-SF	9	8.93	29.724	820
CP-CCSD(T)-SF	9	8.94	29.462	804
CCSD-SF	23	9.15	24.186	742
CP-CCSD-SF	23	9.23	22.882	674
CCSD(T)-SF	23	8.86	28.990	870
CP-CCSD(T)-SF	23	8.93	28.196	749

The perturbative triples, on the other hand, have a substantial impact on the spectroscopic parameters. We therefore restrict the following discussion to results obtained at the CCSD(T) level. A comparison of the spin-free CCSD(T) correlating nine electrons with corresponding calculations including SOC (Table 5) shows that spin-dependent terms are of minor importance for the ground-state spectroscopic parameters. In contrast, both the choice of the basis set and one-particle spinor basis have a significant effect on the equilibrium distance and dissociation energy. Augmentation of the basis set by polarization functions on both atoms (ext_bas) leads to a bond contraction as well as to a bond strengthening. Similar trends are found when the Yb 6p shell is included in the spinor optimization step. Although the CCSD(T) calculations based on a (3in5) averaged spinor basis yield the most attractive potential, the results need to be regarded with caution because of the use of a single-reference method. This choice of one-particle basis is more appropiate for a multireference correlation approach.

The MRCI results for the ground state (Table 6) reproduce very well the spectroscopic values derived from the CCSD(T) calculations. We find a slightly shorter bond and a higher

TABLE 5: Spectroscopic Values for the 1 0.5 Ground State Calculated at the CCSD and CCSD(T) Level with Nine Explicitly Correlated Electrons and Including SOC[a]

method	basis set (av. in DCHF)	corr el	R_e (bohr)	ω_e (cm^{-1})	D_e (cm^{-1})
CCSD-SOC	min_bas (3in 2)	9	9.25	24.073	591
CCSD(T)-SOC	min_bas (3in2)	9	8.98	28.620	795
CCSD-SOC	min_bas (3in5)	9	9.15	25.572	654
CCSD(T)-SOC	min_bas (3in5)	9	8.89	30.214	828
CCSD-SOC	ext_bas (3in2)	9	9.17	24.969	603
CCSD(T)-SOC	ext_bas (3in2)	9	8.90	29.888	826
CCSD-SOC	ext_bas (3in5)	9	9.08	26.443	670
CCSD(T)-SOC	ext_bas (3in5)	9	8.82	31.321	868

[a] The spinor basis was derived from average-of-configurations DCHF calculations, distributing either three electrons in two Kramers pairs (3in2) or three electrons in five Kramers pairs (3in5). A CP correction was not applied.

TABLE 6: Spectroscopic Constants for the Ground and Three Lowest Excited States (Ω Designation) of RbYb Calculated at the MRCI S6_(3in8)_SD Level with Nine Explicitly Correlated Electrons[a]

	state	$\Lambda-\Sigma$[b]	R_e (bohr)	ω_e (cm^{-1})	D_e (cm^{-1})	T_v (cm^{-1})	T_e (cm^{-1})
1	0.5	$^2\Sigma^+$	8.85	29.751	865	0	0
2	0.5	$^2\Pi$	7.40	69.294	7735	7387	5794
1	1.5	$^2\Pi$	7.43	69.322	7164	8104	6581
3	0.5	$^2\Sigma^+$	8.43	52.789	4423	9431	9326
1	0.5(CP)	$^2\Sigma^+$	8.88	29.458	844	0	0
2	0.5(CP)	$^2\Pi$	7.40	69.441	7688	7441	5819
1	1.5(CP)	$^2\Pi$	7.44	69.181	7131	8153	6592
3	0.5(CP)	$^2\Sigma^+$	8.44	52.284	4388	9451	9339

[a] CP-corrected values are given in the lower part of the table. [b] leading $\Lambda-\Sigma$ configuration

dissociation energy of 844 cm^{-1} in relation to the CP-CCSD(T)-SF value of 804 cm^{-1} (Table 4). Typically, CCSD(T) is expected to result in larger binding energies than CI. A thorough analysis of the MRCI wave function reveals, however, substantial multiconfigurational character. The leading configuration consists of a doubly occupied Yb 6s Kramers pair and a bonding orbital composed of Rb 5s and Yb $6p_{1/2}$. In addition, large coefficients are found for single excitations from the bonding orbital as well as double excitations from the Yb 6s shell. The simultaneous occurrence of polarizing and correlating excitations are indicative of the importance of triples as observed in the CC calculations.

From the benchmark calculations on the molecular ground state in connection with a balanced description of the atomic limit (see Table 2) we conclude that with the chosen MRCI setup high accuracy can be achieved for both ground and low-lying excited states.

3.3. Excited-State Potentials. We now discuss in more detail the lower part of the electronic excitation spectrum of the RbYb molecule. Figure 2 displays the calculated potential energy curves for the three lowest excited states corresponding to the atomic Rb $5p_{3/2,1/2}$ and Yb $6s^2_{1/2}$ dissociation channels. The results for the spectroscopic constants of these states are compiled in Table 6 where data are listed with and without a CP correction, respectively.

The three electronically excited states can be divided into two classes, as illustrated in Figure 2. The second state with Ω quantum number 0.5 (denoted in the following by 2 0.5) and the lowest state with $\Omega = 1.5$ (1 1.5) display similar shapes with pronounced potential wells centered around 7.40 bohr (2 0.5) and 7.44 bohr (1 1.5), respectively, and a harmonic frequency ω_e of ca. 69 cm^{-1} derived from the CP-corrected data. Both states are deeply bound with a D_e of 7688 and 7131 cm^{-1}, respectively, whereas the 3 0.5 excited state has a considerably lower binding energy of 4388 cm^{-1}. We find for the latter excited state an equilibrium bond length R_e of 8.44 bohr that is significantly longer compared to the excited states mentioned before but much closer to the minimum internuclear distance of the ground state. This geometric shift is furthermore in agreement with a small difference of ≈112 cm^{-1} between the vertical T_v and adiabatic T_e excitation energies compared to the much larger difference for the other two states.

Comparison of the CP-corrected excited-state spectroscopic constants with their uncorrected counterparts in Table 6 reveals that the excited-state bond distances are less sensitive to basis set superposition errors than the ground-state bond distance. The RbYb bond in the ground state, e.g., decontracts by ≈0.03 bohr upon CP correction whereas the largest shift for an excited state is found to be around 0.01 bohr. Moreover, the adiabatic transition energies T_e are hardly affected by the CP correction with changes of the order of 10−20 cm^{-1}.

3.4. Vibrational Overlaps. Nemitz proposed a two-step mechanism for the production of ultracold RbYb molecules in the rovibronic ground state.[58] Initially, the molecule is prepared in a highly excited rovibrational level close to the dissociation limit of the electronic ground state. Interaction of the molecule with laser light of two different wavelengths promotes RbYb in a first step to some vibrational level of an electronically excited state correlating with the $Rb(^2P) + Yb(^1S)$ atomic levels from which the population is pumped down in a second step to the rovibronic ground state of the molecule. For experimental realization of this scheme, knowledge of the vibrational overlaps between the electronically excited- and ground-state potential wells is of utmost importance. We expect that the dominating difference for a transition probability will be the FCF since all transitions are dipole allowed. We have therefore computed FCFs between vibrational wave functions of the electronic ground state and those of the three lowest electronically excited states. These calculations were perfomed for the ^{87}Rb and ^{176}Yb isotopes since these are favorably employed in experiment.[20]

In Table 7 selected FCFs between the rovibronic ground state (1 0.5, $v = 0$) and vibrational levels of the electronically excited states are listed. (Complete tables of the FCFs are available upon request.) As may be expected from the small geometrical shift between the 1 0.5 and 3 0.5 potential energy wells (see section 3.3), large Franck−Condon overlaps for the lowest vibrational levels of the 3 0.5 state are obtained. For the first excited 2 0.5 as well as the 1 1.5 state significant FCFs are observed for a wide range of vibrational states due to the large spatial extent of the electronic ground state as the maximum amplitude of the $v = 0$ wave function coincides approximately with the outer turning points of these excited-state vibrational wave functions.

FCFs between the calculated highest vibrational state ($v = 69$) of the electronic ground state were found to be on the order of 10^{-4} to 10^{-6} for the 2 0.5, 1 1.5, and 3 0.5 electronic states, as shown in Table 8. Contrary to the situation for the 2 0.5 and 1 1.5 states, none of the vibrational levels of the 3 0.5 state has non-negligible FCFs with the $v = 0$ and $v = 69$ levels of the electronic ground state at the same time. This is, however, a requirement for an effective experimental excitation/deexcitation process.

Our findings thus support a postulated two-step scheme mentioned before aiming at reaching the lowest rovibrational

TABLE 7: Selected Franck−Condon Factors between the Rovibronic Ground State and Vibrationally Excited States (v) of the Electronically Excited States of $^{87}Rb^{176}Yb$

state	v	ΔE (cm^{-1})	FC factor
1 0.5−2 0.5	0	5839	3.4D−11
1 0.5−2 0.5	1	5908	7.8D−10
1 0.5−2 0.5	2	5976	8.9D−09
1 0.5−2 0.5	14	6777	7.1D−03
1 0.5−2 0.5	15	6842	1.1D−02
1 0.5−2 0.5	16	6907	1.7D−02
1 0.5−2 0.5	23	7357	7.5D−02
1 0.5−2 0.5	24	7421	7.8D−02
1 0.5−2 0.5	25	7484	7.7D−02
1 0.5−2 0.5	35	8105	1.2D−02
1 0.5−2 0.5	36	8165	8.1D−03
1 0.5−2 0.5	37	8226	5.6D−03
1 0.5−1 1.5	0	6612	1.0D−10
1 0.5−1 1.5	1	6681	2.2D−09
1 0.5−1 1.5	2	6749	2.4D−08
1 0.5−1 1.5	13	7483	6.4D−03
1 0.5−1 1.5	14	7549	1.1D−02
1 0.5−1 1.5	15	7614	1.6D−02
1 0.5−1 1.5	22	8063	7.6D−02
1 0.5−1 1.5	23	8127	7.9D−02
1 0.5−1 1.5	24	8190	7.8D−02
1 0.5−1 1.5	34	8810	1.2D−02
1 0.5−1 1.5	35	8870	8.1D−03
1 0.5−1 1.5	36	8931	5.5D−03
1 0.5−3 0.5	0	9350	1.5D−01
1 0.5−3 0.5	1	9403	2.3D−01
1 0.5−3 0.5	2	9454	2.3D−01
1 0.5−3 0.5	3	9506	1.7D−01
1 0.5−3 0.5	4	9557	1.0D−01
1 0.5−3 0.5	12	9964	1.2D−04
1 0.5−3 0.5	13	10014	3.9D−05
1 0.5−3 0.5	14	10064	1.3D−05
1 0.5−3 0.5	20	10359	8.0D−09
1 0.5−3 0.5	21	10407	2.2D−09
1 0.5−3 0.5	22	10456	5.7D−10

TABLE 8: Selected Franck−Condon Factors between the Highest Excited Vibrational State (v = 69) of the Electronic Ground State and Vibrationally Excited States (v) of the Electronically Excited States of $^{87}Rb^{176}Yb$

state	v	ΔE (cm^{-1})	FC factor
1 0.5−2 0.5	0	5007	1.7D−04
1 0.5−2 0.5	1	5076	4.9D−05
1 0.5−2 0.5	2	5144	3.1D−05
1 0.5−2 0.5	14	5945	1.2D−05
1 0.5−2 0.5	15	6010	1.5D−05
1 0.5−2 0.5	16	6075	4.3D−05
1 0.5−2 0.5	37	7394	3.4D−05
1 0.5−2 0.5	38	7454	3.5D−06
1 0.5−2 0.5	39	7515	1.4D−05
1 0.5−1 1.5	0	5780	1.9D−04
1 0.5−1 1.5	1	5848	1.5D−05
1 0.5−1 1.5	2	5917	7.1D−05
1 0.5−1 1.5	13	6651	2.8D−05
1 0.5−1 1.5	14	6716	4.1D−06
1 0.5−1 1.5	15	6782	4.5D−05
1 0.5−1 1.5	37	8159	3.4D−06
1 0.5−1 1.5	38	8219	1.4D−05
1 0.5−1 1.5	39	8279	3.7D−05
1 0.5−3 0.5	0	8518	9.6D−15
1 0.5−3 0.5	1	8570	5.8D−14
1 0.5−3 0.5	2	8622	5.1D−16
1 0.5−3 0.5	12	9132	2.7D−05
1 0.5−3 0.5	13	9182	3.3D−05
1 0.5−3 0.5	14	9231	7.9D−06
1 0.5−3 0.5	20	9527	1.4D−04
1 0.5−3 0.5	21	9575	2.0D−05
1 0.5−3 0.5	22	9623	6.3D−05

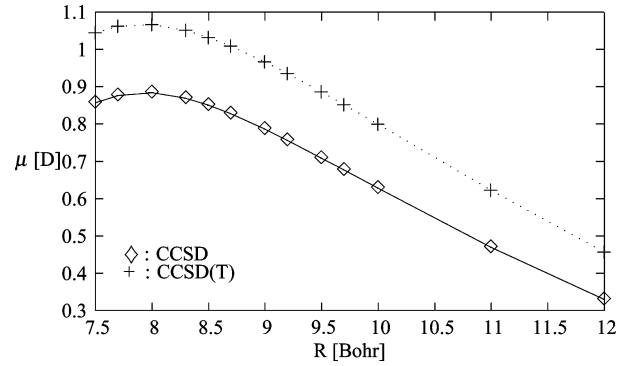

Figure 3. CCSD(T) and CCSD dipole moment curve in Debye with 23 explicitly correlated electrons. The vibrationally averaged dipole moment for CCSD and CCSD(T) is found to be 0.761 and 0.985 Debeye, respectively.

TABLE 9: Dipole Moments at R_e (μ_e) and the Vibrationally Averaged Dipole Moment μ_v for the CCSD and CCSD(T) Levels of Theory with 23 Explicitly Correlated Electrons and with CP Corrected Values

Method	μ_e (D)	μ_v (D)
CCSD-SF	0.763	0.761
CP-CCSD-SF	0.751	0.747
CCSD(T)-SF	0.987	0.985
CP-CCSD(T)-SF	0.977	0.974

level of the electronic ground state.[58] However, we propose to use either the 2 0.5 or 1 1.5 state as intermediate for this process.

3.5. Dipole Moment. Besides having a magnetic dipole moment from an unpaired electron, RbYb also exhibits an electric dipole moment of around 1 D, as illustrated in Figure 3. A fit of the CCSD and CCSD(T) dipole moment curves results in an electric dipole moment of 0.763 and 0.987 D, respectively, at the equilibrium bond distance. A slight decrease of around 0.01 D is observed if the CP correction is added to the ground state, as reported in Table 9. It should be noted that in these cases the dipole moment has not been CP corrected but has been evaluated at the CP-corrected equilibrium bond distance. In Table 9 we have also listed the vibrationally averaged dipole moment, which is only sligthly lower despite the large variation shown by the dipole moment across the rovibrational ground state.

4. Summary and Conclusions

In this study we demonstrate the capability of our relativistic all-electron quantum-chemical methodology to yield accurate ground and excited states on this new and challenging system by approaching the problem in a systematic way. We show that with our chosen MRCI model we are not only able to obtain excellent atomic data but also able to get close to the accurate CCSD(T) data around the equilibrium bond distance of the ground state. We furthermore report spectroscopic constants and Franck−Condon factors for ground and excited states.

Our coupled cluster calculations indicate that RbYb possesses a substantial dipole moment of almost 1 D, thus making it an excellent candidate for the study of dipole−dipole interactions and considering its magnetic dipole moment, making it accessible to magneto-optical trapping. The strongest candidates for reaching the rovibronic ground state via a two-step procedure (after the initial photoassociation), judging from the determined Franck−Condon factors, appear to be the two lowest excited electronic states. For these two states we find reasonable Franck−Condon factors both for the absorption and for the

emission simultaneously. We therefore propose the following two-color process. The longer wavelength laser should excite the molecule to levels with vibrational quantum numbers in the range of $v = 15-35$ in either the 2 0.5 or 1 1.5 potential wells followed by stimulated emission to the rovibronic ground state. This mechanism will give the largest combined Franck−Condon overlap. This picture can, however, change depending on how well the ground state is determined. For example, a shorter equilibrium bond distance for the ground state would favor the first two excited states, whereas a longer one would favor the third excited state. We have therefore performed high-level coupled cluster benchmark studies using a varying number of correlated electrons to calibrate our results.

The inclusion of higher excited states in this molecule necessitates core polarization from Yb 4f5p as these correlate to the atomic $Yb_{6s^16p^1}(^3P_{2,1,0})$ channels, thereby dramatically increasing the computational demand of the problem. Moreover, an accurate description of the $Rb_{4d^1}(^2D_{5/2,3/2})$ atomic limit, which will lie between the $Yb_{6s^16p^1}(^3P_{1,0})$ and $Yb_{6s^16p^1}(^3P_2)$ channels, would require additional higher angular momentum functions to be included in the basis set on Rb. Furthermore, Yb 4f−5d excitations need to be taken into account that are extremely difficult to compute properly. From the methodological aspect one would here also come to the limit of CI because with 31 explicitly correlated electrons size-extensivity errors would likely become sizable. A change to a size-extensive method would then be desirable. Such an approach is currently being investigated by extending the newly implemented general-order four-component multireference coupled cluster[39] to allow for the treatment of excited states.

Acknowledgment. We thank Axel Görlitz and his co-workers for inspiration, for helpful discussions, and for sharing their early findings with us. Financial support of this project by the Deutsche Forschungsgemeinschaft (reference number FL 256/5-1) and through the priority program SPP 1145, grant no. FL 356/2 is gratefully acknowledged. We also thank the Zentrum für Informations- und Medientechnologie (ZIM) at the Heinrich Heine University for providing computational time.

References and Notes

(1) Dulieu, O.; Raoult, M.; Tiemann, E. *J. Phys. B* **2006**, *39* (19).
(2) Cornell, E. A.; Wieman, C. E. *Comput. Phys. Commun.* **2002**, *3*, 476.
(3) Doyle, J.; Friedrich, B.; Krems, R. V.; Masnou-Seeuws, F. *Eur. Phys. J. D* **2004**, *31*, 149.
(4) Hudson, J. J.; Sauer, B. E.; Tarbutt, M. R.; Hinds, E. A. *Phys. Rev. Lett.* **2002**, *89*, 023003.
(5) Regan, B. C.; Commins, E. D.; Schmidt, C. J.; DeMille, D. *Phys. Rev. Lett.* **2002**, *88*, 071805.
(6) Zelevinsky, T.; Kotochigova, S.; Ye, J. *Phys. Rev. Lett.* **2008**, *100*, 043201.
(7) Schiller, S.; Korobov, V. *Phys. Rev. A* **2005**, *71*, 032505.
(8) Stwalley, W. C.; Wang, H. *J. Mol. Spectrosc.* **1999**, *195*, 194.
(9) Weinstein, J. D.; deCarvalho, R.; Guillet, T.; Friedrich, B.; Doyle, J. M. *Nature* **1998**, *395*, 148.
(10) Bethlem, H. L.; Berden, G.; Meijer, G. *Phys. Rev. Lett.* **1999**, *83*, 1558.
(11) Köhler, T.; Góral, K.; Julienne, P. S. *Rev. Mod. Phys.* **2006**, *78*, 1311.
(12) Korek, M.; Allouche, A. R.; Fakhreddine, K.; Chaalan, A. *Can. J. Phys.* **2000**, *78*, 977.
(13) Edvardsson, D.; Lunell, S.; Marian, C. M. *Mol. Phys.* **2003**, *101*, 2381.
(14) Knecht, S.; Jensen, H. J. A.; Fleig, T. *J. Chem. Phys.* **2008**, *128*, 014108.
(15) Le Roy, R. J. *LEVEL, A Computer Program for Solving the Radial Schrödinger Equation for Bound and Quasibound Levels*, Release 8.0; University of Waterloo: Waterloo, CA, 2007; http://leroy.uwaterloo.ca/programs/.
(16) Azizi, S.; Aymar, M.; Dulieu, O. *Eur. Phys. J. D* **2004**, *31*, 195.
(17) Sørensen, L. K.; Fleig, T.; Olsen, J. *J. Phys. B* **2009**, *42*, 165102.
(18) Aymar, M.; Dulieu, O. *J. Chem. Phys.* **2005**, *122*, 204302.
(19) Aymar, M.; Dulieu, O.; Spiegelman, F. *J. Phys. B* **2006**, *39*, S905.
(20) Nemitz, N.; Baumer, F.; Münchow, F.; Tassy, S.; Görlitz, A. *Phys. Rev. A* **2009**, *79*, 061403.
(21) Micheli, A.; Brennen, G. K.; Zoller, P. *Nature* **2006**, *2*, 341.
(22) Tassy, S.; Nemitz, N.; Baumer, F.; Höhl, C.; Batär; Görlitz, A. arXiv:0709.0827v1 [physics.atom-ph], 2007.
(23) Dyall, K. G. *J. Chem. Phys.* **1994**, *100*, 2118.
(24) Eliav, E.; Kaldor, U.; Ishikawa, Y. *Phys. Rev. A* **1995**, *52*, 291.
(25) Eliav, E.; Kaldor, U.; Ishikawa, Y. *Phys. Rev. A* **1994**, *50*, 1121.
(26) Visscher, L.; Dyall, K. G.; Lee, T. J. *Int. J. Quantum Chem.: Quantum Chem. Symp.* **1995**, *29*, 411.
(27) Visscher, L.; Lee, T. J.; Dyall, K. G. *J. Chem. Phys.* **1996**, *105*, 8769.
(28) DIRAC, a relativistic ab initio electronic structure program, Release DIRAC08(2008), written by L. Visscher, H. J. Aa. Jensen, and T. Saue, with new contributions from R. Bast, S. Dubillard, K. G. Dyall, U. Ekström, E. Eliav, T. Fleig, A. S. P. Gomes, T. U. Helgaker, J. Henriksson, M. Iliaš, Ch. R. Jacob, S. Knecht, P. Norman, J. Olsen, M. Pernpointner, K. Ruud, P. Sałek, and J. Sikkema (see http://dirac.chem.sdu.dk).
(29) Fleig, T.; Olsen, J.; Marian, C. M. *J. Chem. Phys.* **2001**, *114*, 4775.
(30) Fleig, T.; Olsen, J.; Visscher, L. *J. Chem. Phys.* **2003**, *119*, 2963.
(31) Fleig, T.; Jensen, H. J.; Olsen, J.; Visscher, L. *J. Chem. Phys.* **2006**, *124*, 104106.
(32) Pitzer, R. M.; Winter, N. W. *J. Phys. Chem.* **1988**, *92*, 3061.
(33) Yabushita, S.; Zhang, Z.; Pitzer, R. M. *J. Phys. Chem.* **1999**, *103*, 5791.
(34) Knecht, S.; Jensen, H. J. A.; Fleig, T. Large-Scale Parallel Configuration Interaction. II.Four-component double-group general active space implementation with application to BiH. *J. Chem. Phys.*, submitted for publication.
(35) Tilson, J. L.; Ermler, W. C.; Pitzer, R. M. *Comput. Phys. Commun.* **2000**, *128*, 128.
(36) Thyssen, J.; Fleig, T.; Jensen, H. J. A. *J. Chem. Phys.* **2008**, *129*, 034109.
(37) Knecht, S.; Jensen, H. J.; Sørensen, L. K. Four-component MP2 natural orbitals: An efficient way of selecting appropiate active spaces for coupled cluster and multiconfigurational self-consistent field calculations, in preparation.
(38) LUCIA, a general CI code written by J. Olsen (University of Aarhus) with contributions from H. Larsen and M. Fülscher.
(39) Sørensen, L. K.; Olsen, J.; Fleig, T. Kramers-Restricted Generalized Active Space Coupled Cluster. Implementation and Initial Application on BiH, manuscript in preparation.
(40) Fleig, T.; Sørensen, L. K.; Olsen, J. *Theor. Chem. Acc.* **2007**, *118*, 347 DOI: 10.1007/s00214-007-0265-y.
(41) Olsen, J. *J. Chem. Phys.* **2000**, *113*, 7140.
(42) Kallay, M.; Surjan, P. *J. Chem. Phys.* **2001**, *115*, 2945.
(43) Auer, A. A.; et al. *Mol. Phys.* **2006**, *2*, 211.
(44) Knecht, S.; Jensen, H. J. A general-purpose parallel four-component Kramers-restricted CI property module, unpublished work.
(45) Gomes, A. S. P.; Dyall, K. G. Manuscript in preparation. Available from the Dirac web site, http://dirac.chem.sdu.dk.
(46) Dyall, K. *J. Phys. Chem. A* **2009**, in press.
(47) Dyall, K. G. *Theor. Chim. Acta* **1998**, *99*, 366.
(48) Pulay, P. Analytical derivative techniques and the calculation of vibrational spectra. In *Modern Electronic Structure Theory, Part II*; Yarkony, D. R., Ed.; World Scientific Publishing Co. Pte. Ltd.: Singapore, 1995; Vol. 2, p 1191.
(49) http://old.iupac.org/reports/periodic_table.
(50) Sioutis, I.; Pitzer, R. M. *J. Phys. Chem. A* **2006**, *110*, 12528.
(51) Halkier, A.; Klopper, W.; Helgaker, T.; Jørgensen, P.; Taylor, P. R. *J. Chem. Phys.* **1999**, *111*, 9157.
(52) Boys, S. F.; Bernardi, F. *Mol. Phys.* **1970**, *19*, 553.
(53) van Duijneveldt, F. B.; van Duijneveldt-van de Rijdt, J. G. C. M.; van Lenthe, J. H *Chem. Rev.* **1994**, *94*, 1873.
(54) Chałasiński, G.; Szczęśniak, M. M. *Chem. Rev.* **2000**, *100*, 4227.
(55) Giese, T. J.; York, D. M. *Int. J. Quantum Chem.* **2004**, *98*, 388.
(56) Laschuk, E. F.; Martins, M. M.; Evangelisti, S. *Int. J. Quantum Chem.* **2003**, *95*, 303.
(57) Lim, I. S.; Lee, W. C.; Lee, Y. S. *J. Chem. Phys.* **2006**, *124*, 234307.
(58) Nemitz, N. *Dissertation, Mathematisch-Naturwissenschaftliche Fakultät*; Heinrich-Heine-Universität Düsseldorf: Düsseldorf, Germany, 2008.
(59) Ralchenko, Yu.; Kramida, A. E.; Reader, J.; NIST ASD Team. *NIST Atomic Spectra Database (version 3.1.5)*; National Institute of Standards and Technology: Gaithersburg, MD, May 3, 2009; http://physics.nist.gov/asd3.

JP904914M